Single-crystal elastic properties of dense hydrous magnesium silicate phase A

CARMEN SANCHEZ-VALLE,[1,]* STANISLAV V. SINOGEIKIN,[1] JOSEPH R. SMYTH,[2] AND JAY D. BASS[1]

[1]Department of Geology, University of Illinois, Urbana, Illinois 61801, U.S.A.
[2]Department of Geological Sciences, University of Colorado, Boulder, Colorado 80309, U.S.A.

ABSTRACT

The single-crystal elastic properties of phase A have been investigated by Brillouin spectroscopy at ambient conditions. The Voigt-Reuss-Hill average for the adiabatic bulk and shear moduli are K_S = 106(1) GPa and μ = 61(1) GPa, respectively. The present acoustic measurements resolve discrepancies between the bulk moduli obtained in earlier compression studies. The axial compressibility of the hexagonal ($P6_3$) structure is highly anisotropic with the c-axis, which is perpendicular to the distorted close-packed layers, approximately 21% stiffer than the a-axis, in agreement with previous compression studies. The hydration of forsterite to phase A decreases the bulk and shear moduli by about 18 and 21%, respectively, while both compressional V_P and shear V_S wave velocities decrease by about 7%. These results suggest that water could be identified seismologically if phase A is present in abundance in cold subducted slabs.

Keywords: Single-crystal elasticity, phase A, Brillouin spectroscopy, water in subduction zones

INTRODUCTION

Dense hydrous magnesium silicates (DHMS) may be hosts for H_2O under hydrous conditions in the Earth's mantle and subduction zones, and their dehydration is a possible cause for deep focus earthquakes (Thompson 1992; Hacker et al. 2003). The DHMS mineral group comprises several complex structures with a wide range of water (2–18 wt%) and silica contents, such as the 10 Å phase (Sclar et al. 1967), the 3.95 Å phase (Rice et al. 1989) or the so-called "alphabet phases" (phase A, B, C, D, E…) (e.g., Frost 1999; Angel et al. 2001). Knowledge of the physical properties of DHMS phases is therefore important for determining their stability field and their relevance for the storage of water in the Earth.

Phase A, which can contain up to 12 wt% water, was first synthesized by Ringwood and Major (1967) and by Sclar et al. (1967) at conditions ranging from 525 to 1100 °C and 7.5 to 18 GPa. The chemical composition of phase A, $Mg_7Si_2O_8(OH)_6$, lies along the forsterite–brucite join (Yamamoto and Akimoto 1974) but its structure differs significantly from that of the humite group. For instance, the crystal structure of phase A consists of two types of layers which are stacked alternately along the direction of the c-axis in a hexagonal array (space group $P6_3$, Horiuchi et al. 1979); the chains of edge-sharing Mg octahedra, which are the key structural units in the humites, are absent.

Phase equilibrium experiments suggest that water can be retained in phase A beyond the dehydration of antigorite and then be carried into the stability fields of phase E and wadsleyite under cool subduction conditions (typically 550 °C at 5.1 GPa) (Luth 1995; Wunder 1998; Komabayashi et al. 2005a). Despite the interest in phase A as a potential carrier of water into the transition zone, substantial uncertainties persist in the determi-

nation of its equation of state and thermodynamic parameters such as the compressibility. Pawley et al. (1995) obtained an isothermal bulk modulus of K_T = 145(5) GPa (assuming K_T' = 4) from energy-dispersive powder diffraction experiments to 9.85 GPa, whereas Crichton and Ross (2002) reported K_T = 97.5(4) GPa with K_T' = 5.97(14) from single-crystal P-V measurements to 7.6 GPa. Later measurements using single-crystal X-ray diffraction by Kudoh et al. (2002) and Kuribayashi et al. (2003) yielded intermediate values of K_T = 105 GPa (assuming K_T' = 4) and 105(4) with K_T' = 3.9(8), respectively. More recently Holl et al. (2006) performed compression experiments in powdered phase A to 33 GPa and reported K_T = 107.2(2.8) GPa with K_T' = 5.7(3). Beyond providing an independent measure of the bulk modulus by a technique other than the static compression methods used thus far, our work is motivated by a lack of any reported information on the shear elastic properties, single-crystal elastic properties, or sound velocity anisotropy of phase A.

To determine the shear elastic properties of phase A and hopefully resolve discrepancies in the previously reported elastic data, we have conducted single-crystal measurements of sound velocities and elastic moduli (K_S and μ) at ambient conditions using Brillouin scattering. In this technique, K_S is obtained without compressing the sample, and the results are not subject to errors that may result from non-hydrostatic conditions or from the fit of the P-V data to a particular equation of state. The results of this study are used to examine the effects of hydration on the elastic properties of phases along the forsterite-brucite mineralogical series, as well as the implication for the seismic low velocity zone within slabs and possibly other areas at depth in the Earth.

EXPERIMENTAL METHODS

The single crystals of phase A used in this study are from the same bulk sample used by Holl et al. (2006) for P-V measurements. They were synthesized from a 1 mm single-crystal cube of San Carlos olivine plus a mixture of brucite and for-

---

sterite sealed in a double platinum capsule and held at 12 GPa and 1200 °C for 3 h using the 5000 ton multi-anvil press of the Bayerisches Geoinstitut (Germany). A detailed description of the synthesis can be found in Holl et al. (2006). The run product consisted of clear single-crystals with lateral dimensions up to 100–150 μm. Both Raman scattering and single-crystal X-ray diffraction (XRD) measurements confirmed the samples to be phase A. The hexagonal unit-cell, space group $P6_3$ (Horiuchi et al. 1979), has lattice parameters: $a = 7.869(4)$ Å, $c = 9.579(4)$ Å, and $V = 513.67$ Å^3. Electron microprobe analyses performed on the sample yielded a chemical composition of $(Mg_{0.981}Fe_{0.019})_7Si_2O_8(OH)_6$ and a water content of 11.9 wt%. A density of 2.976(9) g/cm^3 was calculated from the measured composition and the unit-cell volume.

The elasticity of hexagonal crystals is fully characterized by five independent single-crystal elastic constants (C_{ij} values). Two single-crystals of high optical quality, free of visible inclusions and showing sharp optical extinction were selected for Brillouin experiments. They were ground and polished into 20–25 μm thick platelets with parallel sides and mounted on small goniometers for XRD and Brillouin measurements. Each sample plate was oriented with a four-circle X-ray diffractometer, and then transferred to a three-circle Eulerian cradle for Brillouin experiments. The measured sample plates have normal vectors of (0.4180, 0.9049, 0.0806) and (–0.4681, –0.8836, –0.0128).

Brillouin scattering measurements were performed with a six-pass Fabry-Pérot interferometer using an Argon ion laser ($\lambda = 514.5$ nm) as light source. All spectra were collected in 90° symmetric/platelet scattering geometry, which reduces uncertainties related to the refractive index and the scattering angle. Further details of the Brillouin setup can be found elsewhere (Sinogeikin et al. 1998). Prior to the experiments, the system was calibrated with a standard single-crystal of MgO to minimize systematic errors. Brillouin spectra of phase A were then collected with the laser power kept between 60–70 mW to prevent heating and dehydration of the samples. Typical collection times were 15–20 min, although collection times as long as 10 h were needed to observe the shear acoustic mode with horizontal polarization (V_{SH}). Several polarizations of the incident light were tested without noticeable improvement of the signal. The weak intensity of this mode is the result of the poor phonon-photon coupling in the crystallographic direction contained in the sample planes. However, the measurement of this mode velocity is required to constrain the C_{12} elastic constant in a hexagonal symmetry (Musgrave 1970). All collected Brillouin spectra were of excellent quality with a high signal-to-noise ratio and displayed sharp peaks characteristic of high-quality single crystals (Fig. 1). For each spectrum, the Stokes and anti-Stokes contributions of the compressional (V_P) and shear (V_{SH} and V_{SV}) acoustic peaks were fit assuming Voigt profiles. The accuracy in the determined acoustic velocities is within 0.5%.

RESULTS AND DISCUSSION

The acoustic velocities were measured for each sample plate in 13 distinct crystallographic directions over an angular range of 180°. All spectra showed the compressional (V_P) and one shear mode (V_{SV}), whereas the shear mode with horizontal polarization (V_{SH}) was only observed in spectra with the longest collection times (~10 h) (Fig. 2). The final data set consisted of 57 independent mode velocities, many of which are averages of several redundant measurements in identical directions. We used a least-squares algorithm to calculate the orientations of the phonon directions within the crystallographic plane from the measured acoustic velocities collected on the samples. Acoustic velocities were then inverted to solve for the five independent elastic constants C_{ij} values using a weighted least-squares minimization procedure (Schilling et al. 2003). The best-fit elastic modulus model yields RMS (root mean square) errors of 0.023 km/s with respect to the observed velocities (Table 1). The full data set collected from one of the sample plates is displayed in Figure 2 together with the calculated velocity model from the inversion results.

The sound velocity distribution measured in the samples reveals that phase A has significant shear anisotropy $A_{Vs}[(V_{s,max} - V_{s,min})/V_{s,VRH} = 20\%)]$, with maximum velocity of 5.03(5) km/s in the [–1, 0, –0.669] direction and minimum velocity of 4.10(5)
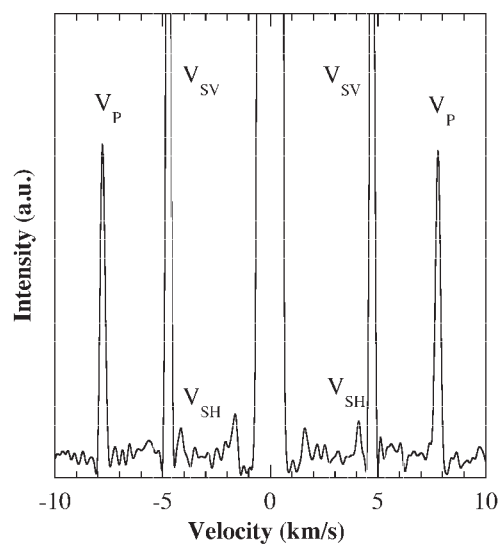

FIGURE 1. Representative Brillouin spectra of phase A at ambient conditions. The features at ±1.7 km/s in the spectrum are unattenuated tails of the Rayleigh peak.
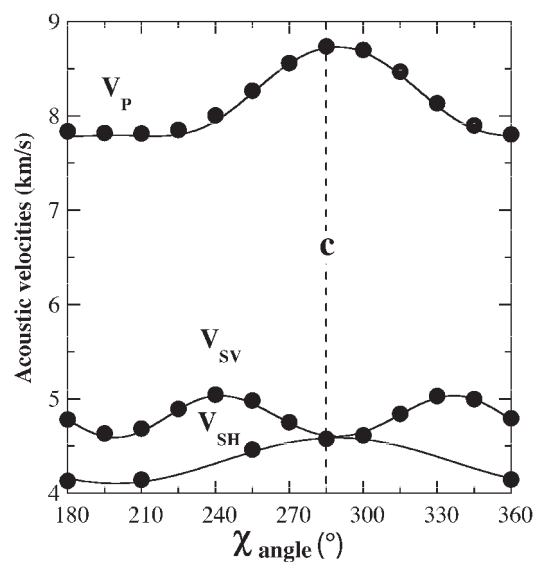

FIGURE 2. Measured acoustic velocities of phase A as a function of the crystallographic direction in the (0.418, 0.9049, 0.0806) crystallographic plane. The best-fit acoustic velocity model is shown by solid lines. Error bars on experimental data are smaller than the symbol sizes.

km/s along the [1 0 0] direction. The longitudinal anisotropy of phase A is less ($A_{Vp} = 12\%$), with maximal velocity of 8.75(9) km/s observed along the [0 0 1] direction (Fig. 2).

The longitudinal moduli (Table 1), C_{11} and C_{33}, indicate significant anisotropy in the axial compressibility of phase A, with the c-axis (C_{33}) being about 21% less compressible than a-axis (C_{11}), in agreement with previous compression studies (Crichton and Ross 2002). This behavior is consistent with a structure composed of two different edge-sharing Mg-octahedra and Si-tetrahedra layers alternating along the c-axis and linked

TABLE 1. Single-crystal elastic moduli and Voigt-Reuss-Hill (VRH) average of the aggregate elastic properties of phase A

C_{ij}	Value (GPa)	Parameter	Value
C_{11}	180.8 ± 1.0	K_s, GPa	106.0 ± 1.0
C_{33}	227.6 ± 2.5	μ, GPa	61.0 ± 1.0
C_{44}	62.7 ± 0.6	V_P, km/s	7.93 ± 0.08
C_{66}	50.1 ± 0.5	V_S, km/s	4.52 ± 0.05
C_{12}	80.6 ± 1.2	V_P/V_S	1.75 ± 0.04
C_{13}	51.2 ± 0.8	σ	0.260 ± 0.005

to each other with strong interlayer bonds (Horiuchi et al. 1979). The aggregate elastic properties of phase A were calculated from the single-crystal elastic moduli C_{ij} values using Voigt-Reuss-Hill (VRH) averaging scheme (Watt and Peselnick 1980). We obtained $K_S = 106(1)$ GPa and $\mu = 61(1)$ GPa for the aggregate bulk and shear moduli, respectively, corresponding to isotropic compressional and shear sound velocities of $V_P = 7.93(8)$ and $V_S = 4.52(5)$ km/s and an aggregate Poisson's ratio $\sigma = 0.260(5)$ (Table 1). The differences between the Voigt and Reuss bounds for the adiabatic bulk modulus of phase A are within 0.13 GPa, whereas the bounds on the shear modulus differ by 2 GPa, due to the significant shear elastic anisotropy.

The isothermal bulk modulus K_T calculated from the Brillouin results (Table 2) is in agreement with the values determined in several previous P-V measurements (e.g., Kudoh et al. 2002; Kuribayashi et al. 2003; Holl et al. 2006). In contrast, our value is 28% lower and 7% higher than the results of Pawley et al. (1995) and Crichton and Ross (2002), respectively (Table 2). The significantly larger K_T of Pawley et al. (1995) may be the result of non-hydrostatic stress developed between grains of the powdered phase A sample and the NaCl pressure standard used in their experiments, as previously suggested by Crichton and Ross (2002). The reason for the apparent discrepancy in the results of Crichton and Ross (2002) is less clear. The difference exceeds the mutual uncertainties in the experimental techniques and is unlikely to be solely explained by the presence of Fe ($X_{Fe} = 0.019$) in our samples. When Crichton and Ross (2002) data are fit by a third-order Birch-Murnagham EoS using the value of K_T derived from the present Brillouin study (104.6 GPa), we obtain a K_T' of 3.4, which is significantly lower than the value reported by the authors. The discrepancy could thus arise from the high degree of covariance between K_T and its pressure derivative K_T' when fitting the P-V data to a particular equation of state, especially over a limited range of compression (Bass et al. 1981). Further Brillouin scattering measurements of the bulk modulus of phase A at high pressure may be required to independently determine the pressure derivative of the bulk modulus.

To assess the effects of hydration on the elastic properties of phases along the forsterite–brucite join, we compared the elastic moduli of phase A with the available Brillouin data for the forsterite-humite system and brucite (Fig. 3a). The adiabatic bulk K_S and shear μ moduli systematically decrease with increasing water content from forsterite to phase A, following trends that can be described by the linear relationships:

$$K_S(\text{GPa}) = 129(1) - 1.85(9) \times \text{wt\% H}_2\text{O} \quad (1)$$
$$\mu(\text{GPa}) = 78(1) - 1.45(14) \times \text{wt\% H}_2\text{O} \quad (2)$$
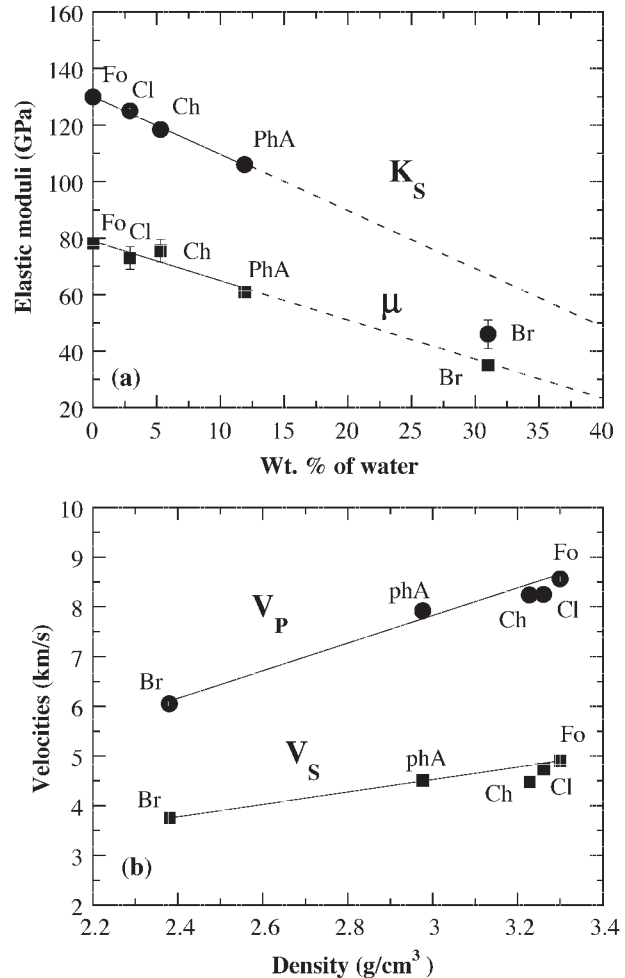
FIGURE 3. Elastic moduli as a function of water content (**a**) and aggregate velocities as a function of density (**b**) for phases along the forsterite–brucite join. Mineral abbreviations and data source are as follows: Fo = forsterite (Zha et al. 1996); Cl = OH-clinohumite (Fritzel and Bass 1997); Ch = chondrodite (Sinogeikin and Bass 1999); PhA = Phase A (this study); and Br = brucite (Xia et al. 1998). Lines are linear fits to the data (solid) and its extrapolation to higher water contents (dashed).

TABLE 2. Isothermal bulk moduli of Phase A, $(\text{Mg}_{1-x}\text{Fe}_x)_7\text{Si}_2\text{O}_8(\text{OH})_6$

| Reference	X_{Fe}	K_T (GPa)	K_T'	Method
Pawley et al. (1995)	0	145(5)	4.0 (fixed)	X-ray powder diffraction (DAC)
Kudoh et al. (2002)	0	105	4.0 (fixed)	Single-crystal X-ray diffraction (DAC)
Crichton and Ross (2002)	0	97.5(0.4)	5.97(14)	Single-crystal X-ray diffraction (DAC)
Kuribayashi et al. (2003)	0	105(4)	3.9(8)	Single-crystal X-ray diffraction (DAC)
Holl et al. (2006)	0.019	107.2(2.8)	5.7(3)	X-ray powder diffraction (DAC)
This study*	0.019	104.6(2.0)	–	Brillouin scattering

Notes: DAC = Diamond-anvil cell.
* The isothermal bulk modulus is calculated from $K_T = K_S/(1 + T\alpha^2 K_S/\rho C_P)$, where $Ks = 106$ GPa and α and C_P are taken from Komabayashi et al. (2005b).

The shear modulus of brucite is consistent with the trend defined by other phases along the join (Xia et al. 1998), whereas its adiabatic bulk modulus is 32% lower than the value predicted from the extrapolation of Equation 1. The linear increase of the compressibility from Fo to phase A may be caused by the progressive reduction in the number of rigid SiO_4 tetrahedral units with respect to the number of weaker octahedral $MgO_4(OH)_2$ units. The absence of tetrathedral units in brucite $Mg(OH)_2$ could account for the dramatic increase of the compressibility. The lack of a consistent trend in K_S vs. H_2O content in Figure 3a emphasizes that the effect of water on elastic moduli may be strongly dependent on the crystal structure and the mechanism of OH^- incorporation (O'Neill et al. 1993; Sinogeikin and Bass 1999). The highly systematic and linear behavior of the shear modulus as a function of H_2O content is surprising to us in this regard. Since the density of minerals is affected by the incorporation of water, this is perhaps a more appropriate variable for measuring the difference between samples. A plot of the aggregate sound velocities as a function of density (Birch 1961) displays clear trends that seem to be independent of crystal structure (Fig. 3b). Both V_P and V_S systematically decrease with decreasing density along the join with slopes of $(dV_P/d\rho) = 2.60(3)$ and $(dV_S/d\rho) = 1.51(2)$ (km.cm³/g.s), respectively.

The hydration of forsterite to phase A decreases the bulk and shear moduli by about 18 and 21%, respectively (Fig. 3a), and produces both compressional V_P and shear V_S wave velocity decreases of 7% (Fig. 3b). These results suggest that water may be readily identified seismologically if phase A is present in abundance at depth in the Earth, and if the velocity trends observed at one atmosphere persist under high-pressure conditions. Thus, the replacement of upper mantle forsterite by phase A could contribute to explain the seismic low velocity zone (LVZ) that has been observed in subduction zones (Helffrich and Abers 1997; Abers 2000).

REFERENCES CITED

Abers, G.A. (2000) Hydrated subducted crust at 100–250 km depth. Earth and Planetary Science Letters, 176, 323–330.

Angel, R.J., Frost, D.J., Ross, N.L., and Hemley, R. (2001) Stabilities and equations of state of dense hydrous magnesium silicates. Physics of the Earth and Planetary Interiors, 127, 181–196.

Bass, J.D., Liebermann, R.C., Weidner, D.J., and Finch, S.J. (1981) Elastic properties from acoustic and volume compression experiments. Physics of the Earth and Planetary Interiors, 25, 140–158.

Birch, F. (1961) The velocity of compressional waves in rocks to 10 kilobars, Part 2. Journal of Geophysical Research, 66, 2199–2224.

Crichton, W.A. and Ross, N.L. (2002) Equation of state of dense hydrous magnesium silicate phase A, $Mg_7Si_2O_8(OH)_6$. American Mineralogist, 87, 333–338.

Fritzel, T.L.B. and Bass, J.D. (1997) Sound velocities in clinohumite, and implications for water in Earth's upper mantle. Geophysical Research Letters, 24, 1023–1026.

Frost, D.J. (1999) The stability of dense hydrous magnesium silicates in earth's transition zone and lower mantle. In Y. Fei, C.M. Bertka, and B.O. Mysen, Eds., Mantle Petrology: Field observations and High-pressure Experimentation, 6, p. 283–296. Geochemical Society Special Publication, Houston, Texas.

Hacker, B.R., Peacock, S.M., Abers, G.A., and Holloway, S.D. (2003) Subduction factory 2. Are intermediate-depth earthquakes in subducting slabs linked to metamorphic dehydration reactions? Journal of Geophysical Research, 108, 2030–2045.

Helffrich, G. and Abers, G.A. (1997) Slab low-velocity layer in the eastern Aleutian subduction zone. Geophysical Journal International, 130, 640–648.

Holl, C.M., Smyth, J.R., Manghnani, M.H., Amulele, G.M., Sekar, M., Frost, D.J., Prakapenka, V.B., and Shen, G. (2006) Crystal structure and compression of an iron-bearing phase A to 33 GPa. Physics and Chemistry of Minerals, in press.

Horiuchi, H., Morimoto, N., Yamamoto, K., and Akimoto, S. (1979) Crystal structure of $2Mg_2SiO_4·3Mg(OH)_2$, a new high-pressure structure type. American Mineralogist, 64, 593–598.

Komabayashi, T., Hirose, K., Funakoshi, K., and Takafuji, N. (2005a) Stability of phase A in antigorite (serpentine) composition determined by in situ X-ray pressure observations. Physics of the Earth and Planetary Interiors, 151, 276–289.

Komabayashi, T., Omori, S., and Maruyama, S. (2005b) Experimental and theoretical study of stability of dense hydrous magnesium silicates in the deep upper mantle. Physics of the Earth and Planetary Interiors, 153, 191–209.

Kudoh, Y., Kuribayashi, T., Kagi, H., Sasaki, S., and Tanaka, M. (2002) High-pressure structural study of phase A, $Mg_7Si_2O_8(OH)_6$ using synchrotron radiation. Journal of Physics: Condensed Matter, 14, 10491–10495.

Kuribayashi, T., Kudoh, Y., and Tanaka, M. (2003) Compressibility of phase A, $Mg_7Si_2H_6O_{14}$, up to 11.2 GPa. Journal of Mineralogical and Petrological Sciences, 98, 215–234.

Luth, R.W. (1995) Is phase A relevant to the Earth's mantle? Geochimica et Cosmochimica Acta, 59, 679–682.

Musgrave, M.J.P. (1970) Crystal Acoustics: Introduction to the study of elastic waves and vibrations in crystals. Holden-Day, Inc., San Francisco.

O'Neill, B., Bass, J.D., and Rossman, G.R. (1993) Elastic properties of hydrogrossular garnet and implications for water in the upper mantle. Journal of Geophysical Research, 98, 20031–20037.

Pawley, A.R., Redfern, S.A.T., and Wood, B.J. (1995) Thermal expansivities and compressibilities of hydrous phases in the system MgO-SiO$_2$-H$_2$O: talc, phase A, and 10-Å Phase. Contributions to Mineralogy and Petrology, 122, 301–307.

Rice, S.B., Benimoff, A.I., and Sclar, C.B. (1989) "3.95" phase in system MgO-SiO$_2$-H$_2$O at pressure greater than 90 kbars: Crystallochemical implications for mantle phases. Abstract International Geological Congress, Washington D.C., meeting 2, 694 (abstract).

Ringwood, A.E. and Major, A. (1967) High-pressure reconnaissance investigations in the system Mg$_2$SiO$_4$-MgO-H$_2$O. Earth and Planetary Science Letters, 2, 130–133.

Schilling, F.R., Sinogeikin, S.V., and Bass, J.D. (2003) Single-crystal elastic properties of lawsonite and their variation with temperature. Physics of the Earth and Planetary Interiors, 136, 107–118.

Sclar, C.B., Carrison, L.C., and Stewart, O.M. (1967) High-pressure synthesis of a new hydroxylated pyroxene in the system MgO-SiO$_2$-H$_2$O. EOS, Transactions of the American Geophysical Union, 48, 226.

Sinogeikin, S.V. and Bass, J.D. (1999) Single-crystal elastic properties of chondrodite: implications for water in the upper mantle. Physics and Chemistry of Minerals, 26, 297–303.

Sinogeikin, S.V., Katsura, T., and Bass, J.D. (1998) Sound velocities and elastic properties of Fe-bearing wadsleyite and ringwoodite. Journal of Geophysical Research, 103, 20819–20825.

Thompson, A.B. (1992) Water in the Earth's upper mantle. Nature, 358, 295–302.

Watt, J.P. and Peselnick, L. (1980) Clarification of the Hashin-Shtrikman bounds on the effective elastic moduli of polycrystals with hexagonal, trigonal, and tetragonal symmetries. Journal of Applied Physics, 51, 1525–1531.

Wunder, B. (1998) Equilibrium experiments in the system MgO-SiO$_2$-H$_2$O (MSH): stability fields of clinohymite-OH [Mg$_9$Si$_4$O$_{16}$(OH)$_2$], chondrodite-OH [Mg$_5$Si$_2$O$_8$(OH)$_2$], and phase A [Mg$_7$Si$_2$O$_8$(OH)$_2$]. Contributions to Mineralogy and Petrology, 132, 111–120.

Xia, X., Weidner, D.J., and Zhao, H. (1998) Equation of state of brucite: Single-crystal Brillouin spectroscopy study and polycrystalline pressure-volume-temperature measurement. American Mineralogist, 83, 68–74.

Yamamoto, K. and Akimoto, S. (1974) High-pressure and high-temperature investigations in the system MgO-SiO$_2$-H$_2$O. Journal of Solid State Communications, 9, 187–195.

Zha, C.-S., Duffy, T.S., Downs, R.T., Mao, H.-K., and Hemley, R.J. (1996) Sound velocities and elasticity of single-crystal forsterite to 16 GPa. Journal of Geophysical Research, 101(B8), 17535–17545.